

Surface fluorination of TiAl particles

* Jae-Ho Kim ¹⁾, Osamu Ogawa²⁾ and Susumu Yonezawa³⁾

¹⁻³⁾ Department of Materials Science & Engineering, University of Fukui, Fukui
910-8507, Japan

¹⁾ kim@matse.u-fukui.ac.jp

ABSTRACT

TiAl alloy particles (30 μ m) could be prepared by the plasma rotating electrode process (PREP) method. Prepared TiAl particles were treated by the surface fluorination using fluorine gas (F₂) at 25 – 200 °C in a pressure of 101 kPa for 3 h. Depending on the reaction temperature, the surface components and structure of TiAl alloy were markedly changed. Below 125 °C, the oxides (TiO₂ and Al₂O₃) existed on TiAl particles was gradually changed into the oxyfluorides (TiOF₂, AlOF etc.). More than 150 °C, the oxyfluorides converted into fluorides (TiF₄ and AlF₃), which were easily hydrolyzed with moisture in air. Regarding the oxidation resistance, the oxyfluorides on the surface of TiAl could restrain less than 0.8 % of weight increase of TiAl particles. However, the fluorides created above 150 °C affected negatively the oxidation resistance. To optimize the beneficial effects of surface fluorination on the oxidation resistance of TiAl alloy, it is necessary to control the F/O contents on the surface.

1. INTRODUCTION

Titanium aluminides based on r-TiAl are considered for high temperature applications in automotive, aerospace and power generation industries [1-5]. Attractive properties such as low density, high stiffness, high yield strength and good creep resistance up to moderately elevated temperature are interesting for the use as structural material in the temperature range between 700 °C and 900 °C. These advantages of TiAl alloys make to partly replace the heavy steels and nickel-based alloys presently used. However, there are still some drawbacks to overcome, such as the limited creep strength and the insufficient oxidation resistance at temperatures above 800 °C. The efforts in the improvement of high temperature oxidation resistance of TiAl include surface modifications and alloying design [6-9]. Many reports indicate that the improvement of oxidation resistance for TiAl favors surface modifications, rather than alloying design [10, 11]. The industrial scale processing routes for TiAl have included ingot casting, powder processing and ingot forging and sheet production by hot-rolling [5, 12]. Powder metallurgy (PM) processing and compaction offers an alternative for prematerial production through hot isostatic pressing (HIP) of TiAl based alloy powder into billets which can be rolled into large sheets [13]. However, the oxide layers such as Al₂O₃ or

²⁾ Graduate Student, ^{1),3)} Professor

TiO₂ on TiAl prevent the sintering of TiAl particles in PM processing. The addition of AlF₃ was reported to improve the sintering properties of Al alloy in PM processing [14-17]. Namely, the AlF₃ reacts with oxide layer formed on Al alloy in the sintering process, and it makes the activation area on the surface of Al alloy powders. Consequently the sintering between activated Al alloy powders could be proceeded by addition of AlF₃.

In this study, we tried to prepare the TiAl powders using PM processing. And the effects of surface fluorination on the oxidation resistance and on TiAl powders were investigated.

2. EXPERIMENTAL DETAILS

Fig.1 shows a total flow diagram for preparation of TiAl powders. Ti powders (>150 μ m, 99.9%) and Al powders (>150 μ m, 99.9%) in ratios of 50:50 was mixed using a pot mill. The mixture was pressed and converted to molded rod (250mm^l x 50mm^φ) under 400 MPa for 3 min. by using the Cold Isostatic pressing (CIP) method. To synthesize TiAl alloy, the prepared molded rod was reacted in vacuum by using the Self-propagating High-temperature Synthesis (SHS) method [18, 19]. TiAl powders (300 μ m) could be prepared from the TiAl rod by using the Plasma Rotating Electrode Process (PREP) method. TiAl powder prepared here was analyzed quantitatively by using SEM/EDX (Ultra-Plus (Carl Zeiss) with XFlash detector 5030(Bruker)). The cross section (200 m) of the TiAl particle was analyzed by ZAF method (automatic PB-ZAF method (Bruker)). The weight ratio of Ti : Al was 31.47 : 68.53 (wt.%), that is 55.10 : 44.90 in atomic percent (at.%). Fluorinated TiAl alloy particles were prepared by direct fluorination using F₂ gas under various reaction conditions. Reaction temperature, fluorine pressure, and reaction time were set at 25–200 °C, 101 kPa, and 3 h, respectively. Details of the fluorination apparatus have been given in our previous paper [20, 21]. The structural and electronic properties of the samples were investigated using powder X–ray diffraction (XRD, Shimadzu; XRD–6100) and X–ray photoelectron spectroscopy (XPS, JEOL; XPS–9010). The surface morphology of various samples was observed using a scanning electron microscope (SEM, s–2400; Hitachi Ltd.). The thermal behavior of TiAl samples was investigated using TG/DTA (Seiko Instruments Inc, TG/DTA 6300) at a heating rate of 10 °C /min up to 1000 °C in air. To prepare the specimen for the mechanical strength, the sample powder was compacted to a rod (55mm^l x 45mm^φ) and pressed at 1000 °C and 180 MPa using HIP (Hot isostatic pressing) method. The tensile test was carried out at 600 °C in Ar gas.

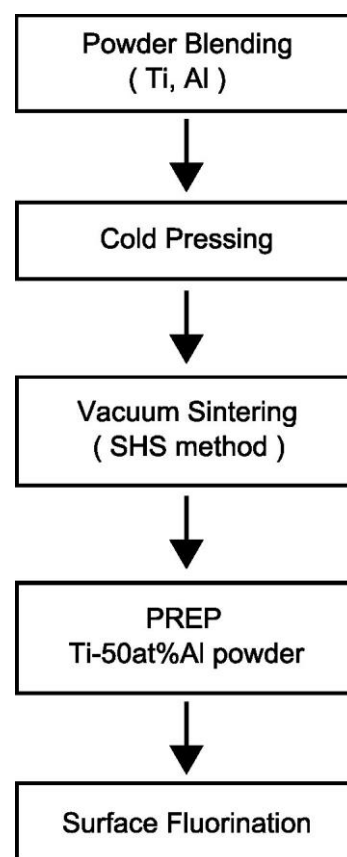


Fig.1 Flow diagram for preparation of TiAl ders.

3. RESULTS and DISCUSSION

Sample names and reaction conditions are summarized in Table 1. SEM images of untreated and fluorinated TiAl samples are presented in Fig. 2. There was no change in

Table 1 Reaction conditions of TiAl particles fluorinated with F₂ gas

Sample name	Temperature (°C)	Time (h)	F ₂ pressure (kPa)
Untreated	-	-	-
F-RT	25	3	101
F-100	100	3	101
F-125	125	3	101
F-150	150	3	101
F-200	200	3	101

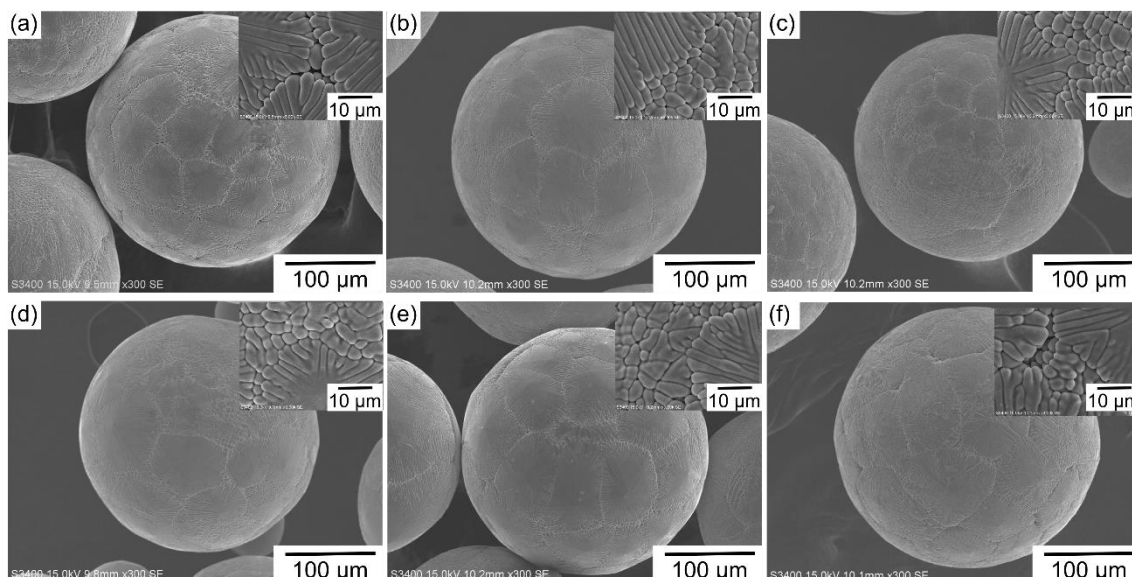


Fig.2 SEM images of various TiAl samples.
 [(a) untreated, (b) F-RT, (c) F-100, (d) F-125, (e) F-150 and (f) F-200]

the shape and the morphology of TiAl particles with these scales along the fluorination. It seems that the contrast of the grain and grain boundary on the particle surface in Fig.2 (a) is observed clearly rather than that for the other samples, Fig.2 (b)-(f). During the SEM observation, the samples after fluorination tend to have the charge up phenomena. So, the electric conductivity of the sample may decrease by fluorination here and the decrease in this electric conductivity may cause the difference in the contrast in the SEM images before and after fluorination. This means the fluorination of TiAl alloy sample didn't cause the change in the morphology but in the electronic state of the sample surface.

Fig. 3 shows XRD profiles of various TiAl samples. The prepared TiAl powders had two profiles of γ -TiAl (\circ) and α_2 -Ti₃Al (Δ). Considering the atomic ratio (55.10 : 44.90) of Ti : Al in TiAl particles calculated with SEM/EDX analysis as shown in experimental part,

γ -TiAl and α_2 -Ti₃Al exists at 8 : 1 in molar ratio in the particle. Below 125 °C of fluorination temperature, there was no extra peak in the profiles. New peaks (◆) were detected near at 35° and 40°, which may be considered as Ti-Al oxyfluorides in case of the F-125 sample. And the intensities of the peaks due to γ -TiAl and α_2 -Ti₃Al decreases at the same time. Especially the peak intensity for α_2 -Ti₃Al decreased largely. It seems

that the surface fluorination of the TiAl particle becomes particular at 125 °C under the reaction condition here. Above 125 °C of fluorination temperature, the peaks of Ti-Al oxyfluorides observed in Fig.3 (d) disappeared. The peaks correspond to γ -TiAl and α_2 -Ti₃Al were clearly detected and S/N ratio of the XRD spectra became small. This may mean that some compounds having low crystallinity may be produced and the inner material part which locates below the oxides surface layer must be exposed. The compounds having low crystallinity must contain some Ti and Al containing fluorides and its decomposition products by the

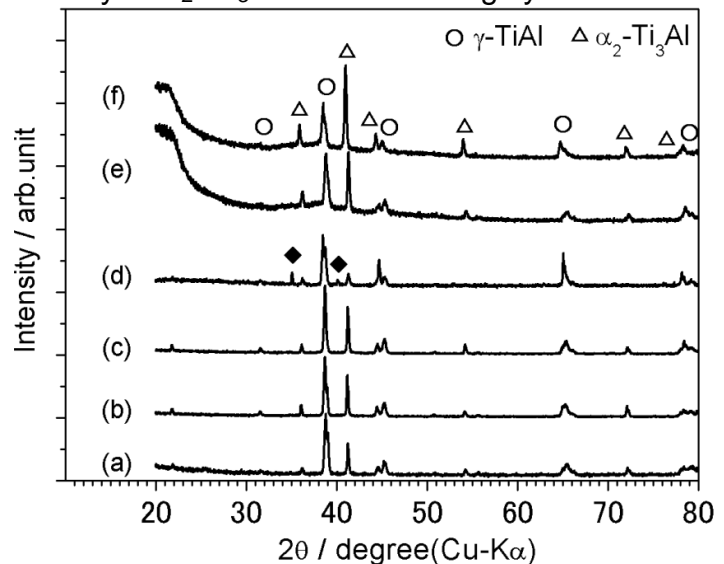


Fig.3 XRD profiles of various TiAl samples.
 [(a) untreated, (b) F-RT, (c) F-100, (d) F-125,
 (e) F-150 and (f) F-200]

reaction with the moisture in the air. The oxyfluorides produced at 125 °C seems to be converted into fluorides by further reaction at the higher temperature.

Fig. 4 indicates XPS spectra of (A) Ti 2p, (B) Al 2p, (C) O 1s, and (D) F1s electrons for untreated and fluorinated TiAl samples. All binding energies were calibrated to the C 1s peak at 284.8 eV of carbon. In case of (A) Ti 2p, the Ti (IV) 2p_{1/2} and Ti (IV) 2p_{3/2} spin-orbital splitting photoelectrons of the untreated TiO₂ (a) were located at binding energies of 464.9 eV and 459.2 eV, respectively. However, in the XPS spectrum after fluorination especially above 125 °C, the peak of Ti 2p_{3/2} shifted to energy higher than that of untreated thing. This result showed that the creation of Ti-F bond of TiOF₂ or TiF₄. Regarding the XPS results of Ti 2p, detailed explanation was indicated in Fig. 5. The Ti 2p peak of F-100 sample was deconvoluted into two separated peaks with Gaussian distributions, as shown in Fig. 5 (a). The peaks located at 459.2 eV and 460.5 eV were attributed to the Ti atom in TiO₂ and TiOF₂, respectively. It means that the TiOF₂ is prepared by the fluorination of TiO₂ on the surface. Furthermore, when the reaction temperature was increased to 125 °C, TiO₂ and TiOF₂ converted into TiOF₂ and TiF₄ with fluorination progressing as indicated in Fig.5 (b). Above 200 °C, however, the appearance of TiO₂ and Ti(III)OF was found with the decreasing of TiF₄ as shown in Fig.5 (c). It may be reasoned for the hydrolysis and sublimation of Ti fluorides such as TiF₄ with moisture in air. In case of Al 2p (Fig.4 (B)), the peak (74.9 eV) of Al₂O₃ shifted to higher energy with the increasing of fluorination temperature. Above 125 °C, the AlF₃ peak was mainly detected near at 77 eV. As similar to the result of Ti 2p, the peak

intensity of AlF_3 was decreased by the hydrolysis with moisture in air. Fig.4 (C) shows the O 1s peaks of various samples. The peak assigned to oxyfluorides was detected at 531 eV in all fluorinated samples (b) – (f). Also, the oxygen contents in surface region of fluorinated TiAl samples were decreased as shown in Table 2. In the F-200 sample, the oxygen contents were obviously increased by the creation of oxyfluorides and/or oxides. In opposite to O 1s, the fluorine contents increased with the increasing of reaction

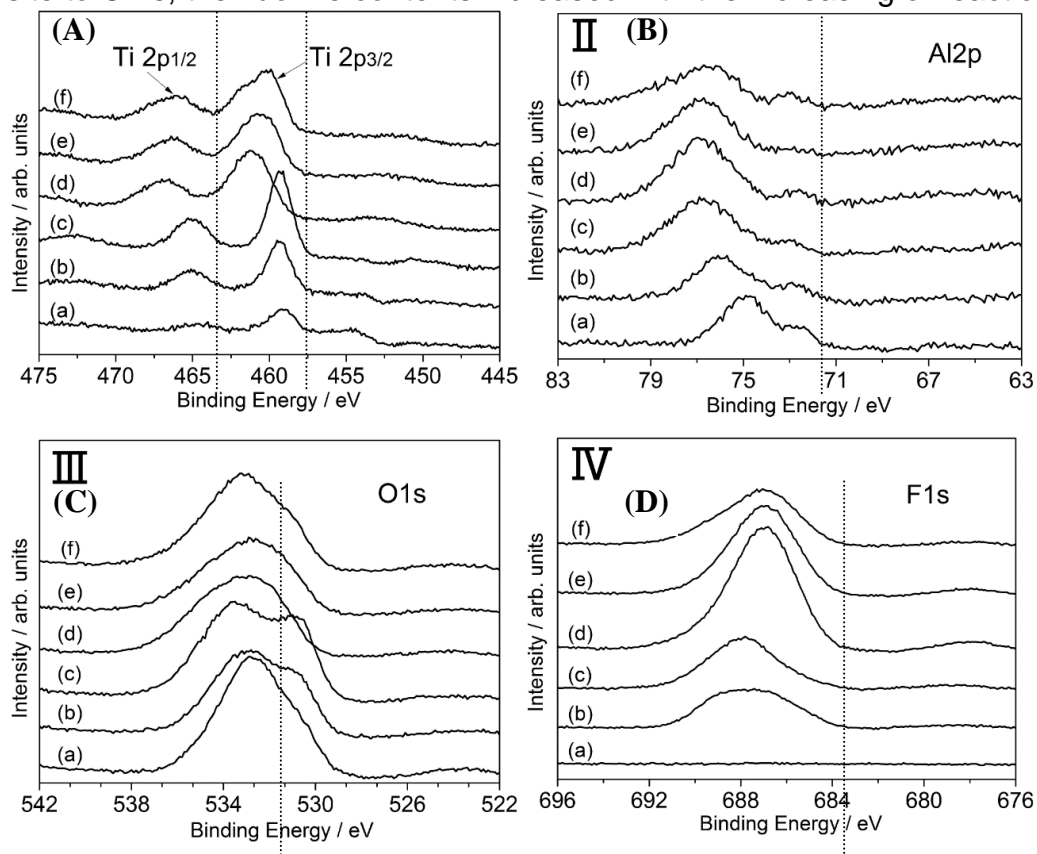


Fig.4 XPS spectra of (A) Ti 2p, (B) Al 2p, (C) O 1s, and (D) F 1s for untreated and fluorinated TiAl particles. [(a) untreated, (b) F-RT, (c) F-100, (d) F-125, (e) F-150, (f) F-200]

Table 2 Elemental contents in TiAl samples evaluated from XPS results (Fig. 4).

sample	Element (atom%)			
	Ti	Al	O	F
untreated	8.69	27.99	63.32	—
F-RT	11.80	16.19	44.07	27.64
F-100C	7.90	21.12	30.69	40.30
F-125	7.12	15.95	20.29	56.64
F-150	6.28	17.37	27.21	49.14
F-200	6.68	16.93	46.35	30.04

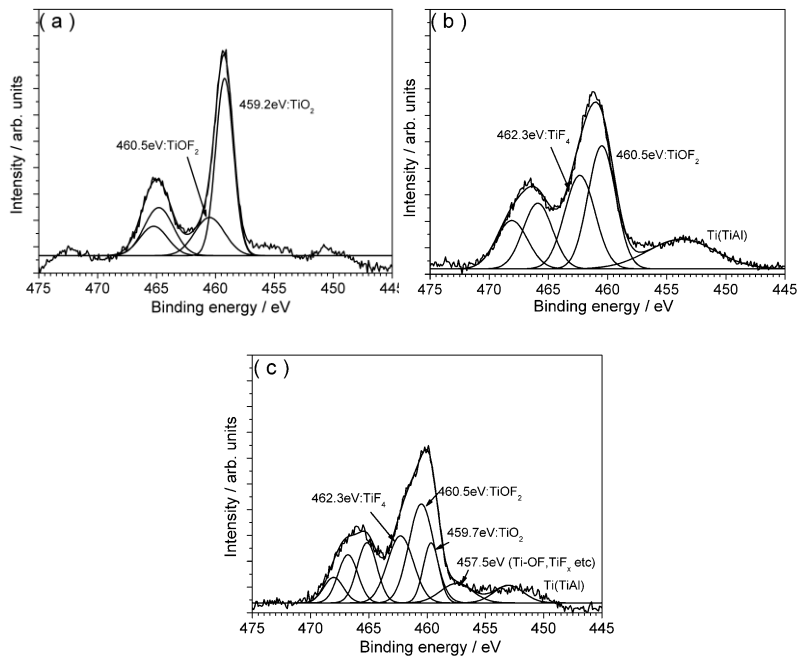


Fig.5 Peak separation of Ti 2p in Fig. 4. [(a) F-100, (b) F-125, (c) F-200]

temperature until 125 °C. More than 125 °C, the fluorine peak (687 eV) assigned to fluorides decreased as shown in Table 2.

To investigate the resistance to oxidation of TiAl alloy, TG/DTA analyses of untreated and fluorinated samples were carried out as shown in Fig. 6 and Fig. 7. Weight change of untreated sample (a) increased drastically more than 800 °C, as shown in Fig.6. It may be reasoned for the formation of oxidation layer by the reaction between metals and oxygen in air. However, the fluorinated TiAl samples could restrain the weight increase even more than 800 °C. Especially, the weight change (< 0.8%) of sample (c) and (d) was much smaller than that (7.2%) of untreated thing. It may be considered that the substantial oxyfluorides on the surface play a role to protect the oxidation of metals. However, in case of sample (e) and (f), the fluorides formed above 150 °C began to be oxidize near at 600 °C, and the weight change reached about 2% at 1000 °C. The exothermic peak of fluorides which caused by oxidation was found at 600 °C in

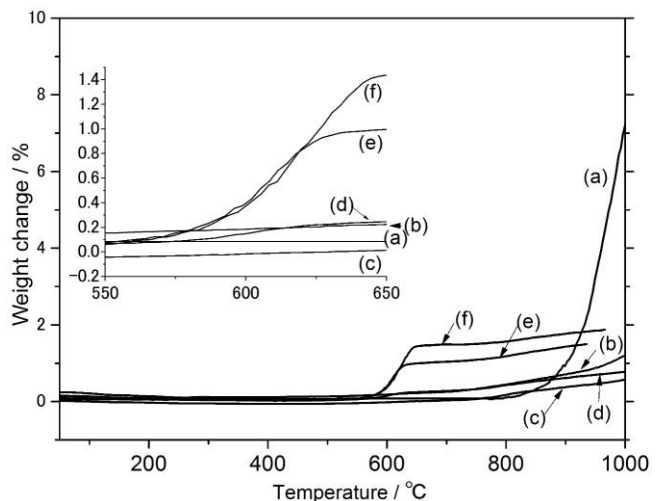


Fig.6 TG curves of various TiAl samples.
 [(a) untreated, (b) F-RT, (c) F-100,
 (d) F-125, (e) F-150, and (f) F-200]

the DTA results, as indicated in Fig. 7. From these results, only oxyfluoride layers on the surface of TiAl are effective for the resistance to oxidation of TiAl alloy.

Fig. 8 shows the SEM images of cross-section of sintered compact in untreated (a) and F-100 (b) samples. At a glance, the sintering particularly proceeds in case of the fluorinated sample. Sphere shape of each TiAl particle has still remained in case of untreated sample while no original shape of the TiAl particle has remained in case of F-100 sample. In addition, there was no void due to the interstitial space of the particle in case of F-100 sample. The surface fluorination could give new potential to TiAl particles as the material for sintering process. The tensile strength of sintered bodies was measured. The sintered bodies made of untreated and fluorinated (F-100) Ti-Al powder have the tensile strength of 314.6 and 407.2 MPa, respectively. That is, F-100 sample exhibited 1.3 times higher tensile strength compared to untreated TiAl sample. Considering the TG data, the sintering must proceed over 900°C.

This greatly influenced on the sintering process and the void-less sintered body can be prepared by using the surface fluorinated Ti-Al powder sample. The fluorination, however, have to be controlled precisely to avoid to over fluorination. Only the oxide layer exist on the surface of the samples have to be fluorinated to improve the sintering property of the sample.

4. CONCLISIONS

We have reported the effects of surface fluorination on the oxidation resistance of TiAl alloy particles. The surface components and structure of TiAl alloy were depended on the reaction temperature. In the range of 25 ~ 125 °C (fluorination temperature), the surface layer on TiAl particles changed from oxides to oxyfluorides. Furthermore, when the fluorination was carried out more than 150 °C, the oxyfluorides converted into fluorides on the surface of TiAl particles. From TG/DTA results, the weight increase (< 0.8% at 1000 °C) of oxyfluorides on TiAl was distinctly smaller than that (7.2 %) of

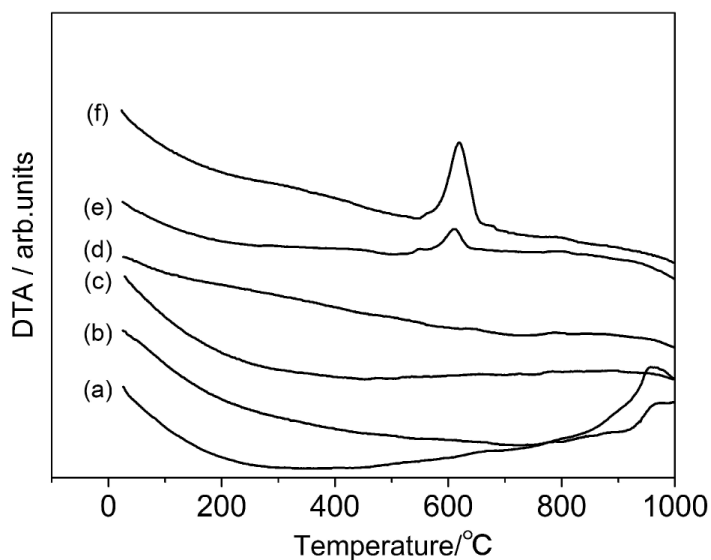


Fig.7 DTA curves of various TiAl samples. [(a) Ti-Al, (b) F-RT, (c) F-100, (d) F-125, (e) F-150, and (f) F-200]

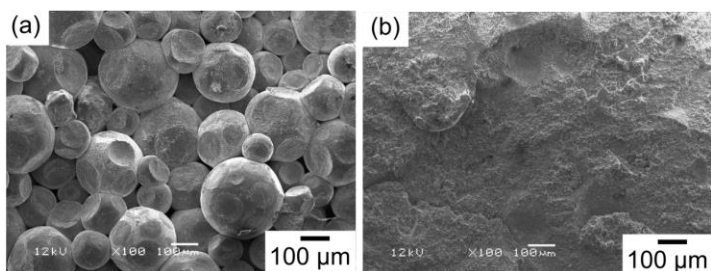


Fig.8 SEM images of cross-section of sintered compact. [(a) untreated and (b) F-100]

untreated TiO₂. However, the weight increase of fluorides was about 2.0 % because of the oxides created from the hydrolysis with moisture in air. Consequently, the controlling of F/O contents such as oxyfluorides on the surface is very effective to make the higher resistance against the oxidation of TiAl particles.

REFERENCES

- [1] K.P.S. Parmar, E. Ramasamy, J.W. Lee, J.S. Lee (2010), "A simple method for producing mesoporous anatase TiO₂ nanocrystals with elevated photovoltaic performance", *Scripta Materialia*, **62**, 223–227.
- [1] W.J. Zhang, B.V. Reddy, S.C. Deevi (2001), *Scripta Mater.*, **45**, 645–651.
- [2] M. Yamaguchi, H. Inui, K. Ito (2000), *Acta Mater.*, **48**, 307–322.
- [3] T. Tetsui, S. Ono (1997), *Intermetallics*, **7**, 689–697.
- [4] T. Noda, *Intermetallics* 6 (1998) 709–713.
- [5] H. Clemens, H. Kestler (2000), *Adv. Eng. Mater.*, **2**, 551–570.
- [6] M.R. Yang, S.K. Wu (2002), *Acta Mater.*, **50**, 691–701.
- [7] I.C. Hsu, S.K. Wu, R.Y. Lin (1997), *Mater. Chem. Phys.*, **49**, 184–190.
- [8] J.P. Kim, H.G. Jung, K.Y. Kim (1999), *Surf. Coat. Technol.*, **112**, 91–97.
- [9] Z. Tang, L. Niewolak, V. Schemet, L. Singheiser, W.J. Quadarkker, F. Wang (2002), *Mater. Sci. Eng. A*, **328**, 297–301.
- [10] J.K. Lee, M.H. Oh, D.M. Wee (2002), *Intermetallics*, **10**, 347–352.
- [11] C. Zhou, Y. Yang, S. Gong, H. Xu (2001), *Mater. Sci. Eng. A*, **307**, 182–187.
- [12] H. Clemens (1995), *Z Metallkd*, **86**, 814–822
- [13] F. Appel, U. Brossman, U. Christoph, S. Eggert, P. Janschek, U. Lorenz (2000), *Adv. Eng. Mater.*, **2**, 699–720.
- [14] S.Masuoka, Y.Arami, S.Nagai (2002), *J. Jpn. Soc. Powder Metallurgy*, **49**, 1003–1008.
- [15] M. Ohtsuki, T. Kohni (1989), *J. Jpn. Soc. Powder Metallurgy*, **36**, 723–726.
- [16] S. Masuoka, Y.Arami (2007), *J. Jpn. Soc. Powder Metallurgy*, **55**, 64–66.
- [17] T. Inaba, S.Nagai, O. Iwatsu, N. Nakanishi, T. Shigematsu (1989), *J. Jpn. Soc. Powder Metallurgy*, **36**, 149–152.
- [18] B. Aminikia (2012), *Power Technology*, **232**, 78-86
- [19] J. Guojian, X. Jiayue, Z. Hanrui, L. Wenlan (2011), *Materials Letters*, **65**, 2969-2971
- [20] M. Takashima, Y. Nosaka, T. Unishi (1992), *Eur. J. Solid State Inorg. Chem.*, **29**, 691–703.
- [21] J.H. Kim, H. Umeda, M. Ohe, S. Yonezawa, M. Takashima (2011), *Chem. Lett.*, **40**, 360-361.